



Published in final edited form as:

*Nat Nanotechnol.* 2019 July ; 14(7): 645–657. doi:10.1038/s41565-019-0487-x.

## An atlas of nano-enabled neural interfaces

Héctor Acarón Ledesma<sup>1,2</sup>, Xiaojian Li<sup>3,4</sup>, João L. Carvalho-de-Souza<sup>5,10</sup>, Wei Wei<sup>6</sup>,  
Francisco Bezanilla<sup>2,5,7</sup>, Bozhi Tian<sup>2,8,9,\*</sup>

<sup>1</sup>Graduate Program in Biophysical Sciences, University of Chicago, Chicago, IL, USA.

<sup>2</sup>Institute for Biophysical Dynamics, University of Chicago, Chicago, IL, USA.

<sup>3</sup>Brain Cognition and Brain Disease Institute of Shenzhen Institutes of Advanced Technology, Chinese Academy of Sciences, Shenzhen, People's Republic of China.

<sup>4</sup>Shenzhen-Hongkong Institute of Brain Science, Shenzhen, People's Republic of China.

<sup>5</sup>Department of Biochemistry and Molecular Biology, University of Chicago, Chicago, IL, USA.

<sup>6</sup>Department of Neurobiology, University of Chicago, Chicago, IL, USA.

<sup>7</sup>Centro Interdisciplinario de Neurociencias, Facultad de Ciencias, Universidad de Valparaíso, Valparaíso, Chile.

<sup>8</sup>Department of Chemistry, University of Chicago, Chicago, IL, USA.

<sup>9</sup>James Franck Institute, University of Chicago, Chicago, IL, USA.

<sup>10</sup>Present address: Department of Anesthesiology, University of Arizona College of Medicine, Tucson, AZ, USA.

### Abstract

Advances in microscopy and molecular strategies have allowed researchers to gain insight into the intricate organization of the mammalian brain and the roles that neurons play in processing information. Despite vast progress, therapeutic strategies for neurological disorders remain limited, owing to a lack of biomaterials for sensing and modulating neuronal signalling in vivo. Therefore, there is a pressing need for developing material-based tools that can form seamless biointerfaces and interrogate the brain with unprecedented resolution. In this Review, we discuss important considerations in material design and implementation, highlight recent breakthroughs in neural sensing and modulation, and propose future directions in neurotechnology research. Our goal is to create an atlas for nano-enabled neural interfaces and to demonstrate how emerging nanotechnologies can interrogate neural systems spanning multiple biological length scales.

---

Reprints and permissions information is available at [www.nature.com/reprints](http://www.nature.com/reprints).

\*Correspondence should be addressed to B.T. btian@uchicago.edu.

Competing interests

The authors declare no competing interests.

Additional information

**Publisher's note:** Springer Nature remains neutral with regard to jurisdictional claims in published maps and institutional affiliations.

Understanding the working principles of the nervous system has been a major goal of modern biomedical research. The brain is a high-dimensional functional network that accommodates around 100 billion neurons (in humans) which form local and long-range connections that drive processing of information in specialized brain centres and establish communication across systems, respectively. The complexity of the mammalian brain arises from three important phenomena. First, the high dimensionality of the vertebrate brain creates a ‘big data problem’ for neuroscience research. Second, neuronal subcellular structures span various length scales, such as tens of nanometres for synapses to centimetres for axonal projections, making it difficult to probe these components simultaneously with current technologies. Finally, approximately another 100 billion non-neuronal cells, called glia, reside in the brain and regulate neural activity through mechanisms that are still poorly understood.

### Importance of nanoscale for neuronal interfaces

Historically, breakthroughs in neuroscience research have been tied to technological advances. For instance, bioelectric phenomena were first explored in the 1790s by Luigi Galvani, but it was not until the advent of electrophysiological recordings in the mid-twentieth century that theories of membrane excitability and ion channels were properly formulated. More recently, the design of new molecular tools for neuromodulation has provided scientists with the ability to control the activity of defined populations of neurons and to establish links between neural pathways and behaviour<sup>1</sup>. Nevertheless, our understanding of brain function remains poor, and our ability to prevent and treat neurological disorders is limited, in part because of the lack of minimally invasive tools capable of probing neuronal systems across the range of spatiotemporal scales. Currently, medical professionals rely on bulky implantable metal electrodes to pinpoint the origin of seizures, alleviate symptoms of Parkinson’s disease and stimulate nerve growth following injury. The large size of these electrodes relative to individual cell bodies and nerve fibres leads to the activation of surrounding neurons during stimulation, creating unwanted side-effects<sup>2</sup>. Additionally, mechanical insertion of these bulky microelectrodes combined with micromotions within the skull<sup>3</sup> leads to immune activation and glial scar formation<sup>4</sup>, which encapsulates the electrode, causes displacement from neurons of interest, decreases the overall device performance and even remodels the structure and function of the neural network surrounding the electrode.

Motivated by increasing demand, academic, federal and private sectors have expanded their research efforts in neural technologies. For instance, the BRAIN Initiative<sup>5</sup> in the United States, the Human Brain Project<sup>6</sup> in the European Union and the China Brain Project<sup>7</sup> are all multi-billion dollar projects that aim to develop new technologies, build seamlessly integrated neural interfaces for the interrogation of neural signals in freely moving and socially active subjects (Fig. 1a), and design personalized electronic medicine.

Nanoscale biomaterials can circumvent the limitations of current technologies, representing a potential imperceptible platform (Fig. 1a) for interfacing the nervous system at unprecedented spatiotemporal scales. First and foremost, the use of nanoscale building blocks means that electrodes can be packed together more densely, improving the resolution

of current recording and neuromodulatory systems. Furthermore, given that bending stiffness scales with the cube of material thickness<sup>8</sup>, rigid materials become soft, flexible, stretchable and more biocompatible as their feature size reaches the nanoscale (Fig. 1a–c), reducing the mechanical mismatch between brain tissue and engineered materials. Therefore, although the overall size of implantable devices may remain at the macroscopic scale, nanoscale building blocks that mimic structural and mechanical properties of neural tissue can be seamlessly integrated with brain tissue, without being recognized by the immune system<sup>9</sup>. Indeed, multiple lines of evidence have demonstrated that neural tissue exhibits negligible glial activation and scar formation when implanted with devices fabricated from nanoscale mechanically compliant subunits<sup>10</sup> (Fig. 1b, right). Additionally, scaling down to the nanoscale can yield new physical properties and improved device capabilities, partially because the chemical, mechanical, thermal and electrostatic energies all converge at the nanoscale (Fig. 1c), aiding signal transduction across different energy terms<sup>11</sup>. For instance, atomically thin nanoscale materials that can harvest electromagnetic radiation energy in the Wi-Fi band have been reported, making it possible to actuate neural implants by means of everyday electronics<sup>12</sup>. Also, nanostructures display size- and shape-dependent plasmonics and photoluminescence, superparamagnetism, enhanced electronic properties and bioactive topographical features, all of which are suitable for neural interrogation (Fig. 1d). The energy-matching phenomenon (Fig. 1c) and the emergence of new properties at the nanoscale (Fig. 1d) can lead to innovative modes of sensing and stimulation that would not be possible with bulky materials or devices.

Finally, nanoscale materials and devices enable localized neural probing. Neuronal membranes and subcellular compartments (Table 1) represent extremely crowded environments that use nanoscale molecular machinery to execute numerous tasks in parallel (Fig. 1e). For example, previous research has illustrated how cellular and biomolecular interactions along with the electrical properties of neuronal membranes formulate the classical description of synaptic transmission (Fig. 1e). However, how the surrounding local microenvironment, including intimately associated astrocytes, the extracellular matrix, and nearby neuronal processes, influences neural communication is a topic of active research that would benefit from tools with improved spatial resolution and cellular/subcellular targeting. Furthermore, neurons receive synaptic inputs across their dendritic trees, where the summation and integration of local excitatory and inhibitory inputs result in deviations from the resting potential; and, while in most neurons action potentials are generated at the axon hillock, their dendrites are also capable of nonlinear transformations of electrical signals. In addition, biological membranes experience limited propagation of mechanical tension<sup>13</sup> and can therefore elicit localized intracellular signalling in cellular subunits. Thus, nanoscale tools that depict a more accurate description of the multimodal signals experienced by cellular subunits would provide a better interpretation of neuronal input–output relationships and of electrical and mechanical heterogeneities (Fig. 1f). Moreover, if delivered intracellularly, nanoscale devices would be capable of real-time interrogation of signalling complexes and subcellular organelles — including the cytoskeleton, mitochondria and endoplasmic reticulum (Fig. 1e) — allowing scientists to explore their contributions to neural activity and determine protocols for rescuing neural phenotypes during disease.

## Natural and cultured neural systems

During development, neurons assemble into functional networks through the concerted action of both molecular<sup>14</sup> and activity-dependent<sup>15</sup> mechanisms. The precise organization of excitatory and inhibitory synapses in local brain circuits coordinates the algorithmic functions involved in the execution of complex tasks such as information processing. In the case of the vertebrate retina, the way in which neurons organize throughout development gives rise to its characteristic laminar structure (Fig. 2a), determines the direction of information flow<sup>16</sup> and dictates the termination patterns of retinal axons onto downstream visual nuclei. Photoreceptors, bipolar cells and retinal ganglion cells form the main excitatory pathway in the retina and transmit information vertically<sup>16</sup> (Fig. 2a), whereas horizontal cells and amacrine cells provide lateral inhibitory input to retinal neurons, helping to regulate the extent to which membranes become depolarized and thus modulate neuronal output. Because most circuit motifs observed throughout higher-order brain centres can be found in this simple tissue (three cellular layers and two synaptic layers), the retina has become a model system for testing developing neural technologies and for understanding how to restore sensation and proper neural function. For example, optoelectronic retinal prostheses, or devices capable of converting light into electrical currents that can activate the retinal network<sup>17</sup>, are currently being explored as avenues for restoring vision. Although these have been effective as proof-of-concept, scaling down building block components to the nanoscale<sup>18</sup> (blue dots in Fig. 2a) may further enhance properties at the biointerface and even offer new interrogation capabilities. For example, injectable mesh nanoelectronics have enabled long-term in vivo recordings from individual retinal ganglion cells in awake animals<sup>19</sup>, a capability previously inaccessible with conventional devices. More recently, injectable self-powered near-infrared (NIR) nanoantennae based on up-conversion nanoparticles (UCNPs) that bind to photoreceptors and transform NIR light into short-wavelength emissions have extended the mammalian visual spectrum into the NIR range<sup>20</sup>. Lastly, besides subretinal and epiretinal implantation, nanoscale electrodes may interface subcellular structures in the inner retina, such as dendritic shafts and individual varicosities, allowing compartmentalized signalling to be studied and shedding light on how information is processed by neuronal subunits.

Brain structures and neural signals (Table 1) are complex, multiscale and highly interconnected, and are regulated by many nonneuronal factors, including glial interactions and the extracellular matrix. For over a century, scientists have relied on cultured systems (Fig. 2b–d) to gain access to specific cell types and to simplify experimental studies. While primary cell cultures of hippocampal, cortical, and spinal cord neurons have been instrumental in elucidating mechanisms underlying neuronal development and cell polarization<sup>21</sup>, these cannot recapitulate many key extrinsic factors and signals that are known to coordinate neuronal organization, synaptogenesis and circuit development<sup>22</sup>.

Advances in microfabrication and stem cell biology have led to the implementation of new in vitro model systems that can simplify and accelerate the characterization of nanoscale tools for neuroscience (blue dots in Fig. 2b–d). For example, immature neurons have been cultured in elastomeric polydimethylsiloxane (PDMS) microchips, in which channels and chambers provide spatiotemporal control of the extracellular chemical environment<sup>23</sup> (Fig.

2b). A similar approach can be used to study the formation of synapses between neuronal populations and the associations between neurons and glial cells<sup>24</sup> (Fig. 2b). Nanoscale devices can be used in conjunction with these microfluidic systems to study axogenesis, myelination and synaptogenesis.

Recently, three-dimensional (3D) co-cultures and brain organoids have emerged as other in vitro alternatives that address some of the limitations experienced with 2D primary cell cultures<sup>25,26</sup>. For example, neurons assembled into cortical spheroids (Fig. 2c) display an enhanced level of self-organization reminiscent of a developing neocortex and exhibit molecular expression of both deep and superficial cortical biomarkers<sup>27</sup>. Therefore, neurospheroids derived from human-induced pluripotent stem cells (hiPSCs) can more faithfully recapitulate human brain physiology<sup>26–28</sup> and have potential as neural models for studying the pathophysiology and progression of neuropsychiatric disorders. Stitching together blocks of tissue containing distinct neuronal populations (Fig. 2c) allows the study of attraction and repulsion of self and non-self neurites during synaptogenesis and of how they establish wiring specificity<sup>29</sup>. Nanoscale materials could probe the role played by local bioelectric signals during this process. Similarly, brain organoids grown from differentiated hiPSCs have become attractive models for studying brain development. As originally described by Eiraku et al., brain regions can spontaneously sprout from embryoid bodies, or clusters of embryonic stem cells, simply by modifying the conditions and local microenvironment in which cells are cultured<sup>30</sup>. Further work on brain organoids has realized retina-like<sup>25</sup> and forebrain-like structures<sup>25,28,31</sup> with neurons becoming integrated into spontaneously active networks and photosensitive neurons in the optic cup enabling coordinated evoked activity upon light illumination<sup>25</sup>. Nanoscale devices can interface brain organoids as they differentiate and develop into specialized brain regions, allowing scientists to understand how bioelectric signals emerge in the developing brain and how neural networks transition between activity states during development.

## Nanoscale tools and building blocks

Current tools for neural interrogation include single-unit pulled glass micropipette electrodes or multi-electrode arrays, such as the Utah- and Michigan-style arrays. However, their mechanical invasiveness and the decaying signal-to-noise ratio has pushed further research to focus on the miniaturization of these technologies and the innovation of platforms capable of seamless integration with brain tissue.

### Substrate-bound transistors

Semiconductor nanostructures have emerged as promising materials for next-generation neural interfaces owing to their diverse physical properties, scalable fabrication and good biocompatibility<sup>32</sup>. In particular, nanoscale field-effect transistors (nanoFETs) represent a powerful alternative to traditional platforms because their performance does not depend on device impedance and can be experimentally scaled down to the sub-10-nm regime<sup>33</sup>. Of particular relevance to neuroscience applications, carriers in the transistor channel of nanoFETs can be depleted (or modulated) by neural signals much more easily than in bulk, yielding higher voltage sensitivity<sup>34</sup> (Fig. 1d). Additionally, the intrinsic delay time of a

FET, as described either by equation (1) for conventional complementary metal–oxide semiconductor or by equation (2) for junctionless nanowire FETs

$$\tau \approx \frac{L^2}{\mu V_{DD}}$$

(1)

$$\tau \approx \frac{C_{ox} L^2}{q\mu N_D T_{Si}}$$

(2)

(where  $C_{ox}$  the gate oxide capacitance,  $L$  is the transistor gate length,  $\mu$  the electron mobility,  $N_D$  the doping concentration,  $T_{Si}$  the thickness of silicon and  $V_{DD}$  the supply voltage)<sup>35</sup> implies that with decreasing  $L$ , the device speed increases, potentially allowing nanoFETs to resolve faster neural events. Novel nanoFET configurations have been introduced in the past decade (Fig. 3a), including those based on kinked nanowires<sup>36</sup>, bent nanowires<sup>37</sup>, Si nanowire backbone/oxide nanotube branch structures<sup>33,38</sup>, Si nanotubes<sup>39</sup>, ultra-short channel and etched nanowires<sup>40</sup>, nanomembranes<sup>41</sup>, porous particles<sup>42</sup> or graphene<sup>43,44</sup>, and those integrated into mesh-like nanoelectronics<sup>45–47</sup>. Additionally, stretchable, high-mobility transistors have been realized by exploring nano-confinement in semiconducting polymers<sup>48</sup>. Many of these nanoFETs act as point-like detectors capable of recording the dynamics of membrane voltages and extracellular field potentials. Furthermore, design principles have been developed for the future implementation of nanoFETs in either chronic<sup>10,49</sup> or transient<sup>41,50</sup> applications.

### Substrate-bound electrodes

A common strategy for reducing electrical impedance and improving charge injection capability is to enhance the surface area by introducing roughness, porosity or other nanostructured<sup>51,52</sup> topographies to metal electrodes (Fig. 1d). Over the past decade, engineering approaches have been developed to expand the scope of miniaturized and nanostructured metal electrodes.

First, an important step has been the achievement of intracellular or intracellular-like recordings (Fig. 3b). For instance, mushroom-shaped noble-metal electrodes help in the detection of intracellular signals following engulfment through intrinsic phagocytic pathways<sup>53,54</sup>. Similarly, vertical metal nanopillars<sup>55</sup>, nanotubes<sup>56</sup> and metal-coated semiconductor nanowires<sup>57</sup> have demonstrated the capacity for intracellular recording and stimulation following electroporation. Gold nanotubes have also been used for localized

poration (that is, pore formation in membranes) upon irradiation with near-infrared laser pulses, which allows for multiplexed intracellular recordings in neurons<sup>58</sup>. Following this logic, nanoporous (50–200 nm) thin films of Pt metal have been used in the design of ultrasensitive electrodes for the recording and stimulation of excitable membranes following optoacoustic poration<sup>59</sup>.

Second, considerable advances have been achieved in the fabrication of nanostructured electrode arrays over flexible or even macroporous polymer substrates<sup>45,47,49</sup> to create mechanically compliant 2D or 3D interfaces (Figs. 1a, 3b). Besides 3D mesh nanoelectronics, Xie and colleagues embedded Pt and Au electrodes in an ultraflexible polymer shank to create one of the smallest neural probes ever reported, the nanoelectronic thread<sup>60</sup>.

Finally, integrated approaches have been developed to incorporate neural electrodes into other device platforms, such as microfluidic systems. For example, metal nanoelectrodes suspended from microfluidic channel walls (nanospears) have been used to study neuromuscular signal transduction<sup>61</sup> in intact small animals.

### Free-standing organic nanostructures

Untethered operation of nanostructured platforms is attractive, as it allows these materials to act as free-standing devices and enables wireless interrogation of cellular activity through recording or localized stimulation (Fig. 3c). Nanostructured biological materials<sup>62–70</sup> fabricated through rational design have ideal properties for subcellular interrogation, given their natural occurrence in biology, nanoscale feature size and self-assembly. For example, the incorporation of responsive domains and functional moieties into self-assembled DNA nano-constructs provides a powerful approach for fabricating devices capable of sensing and actuation, as recently exemplified in sensors for ionic species<sup>62,65</sup>, in lysosome sensors based on fluorescence resonance energy transfer<sup>66</sup> and in drug-delivery vectors<sup>67</sup>. Other forms of nanostructured biological materials, such as peptide-presenting nanostructures<sup>68</sup>, exosomes<sup>69</sup> and bacterial gas vesicles<sup>70</sup>, are now beginning to be exploited as biological probes. In particular, gas vesicles —gas-filled protein-shelled compartments with typical widths of 45–250 nm and lengths of 100–600 nm — can help the cavitation centre to transduce acoustic energy into mechanical force or boost the functional ultrasound imaging resolution. Finally, besides polymer nanostructures<sup>71,72</sup>, synthetic molecular machines<sup>73</sup> designed as rotors, walkers and cages have been used to transform optical energy into mechanical action causing reversible or irreversible openings in the lipid bilayer<sup>74</sup>.

### Free-standing inorganic nanostructures

Optical<sup>75</sup>, acoustic<sup>76</sup> and magnetic stimulation<sup>77</sup> represent non-invasive methods for neural stimulation. However, these strategies alone do not show optimal spatial resolution, lack ways of selective targeting and often require high power densities potentially causing off-target effects. On the other hand, inorganic nanoscale materials are capable of harnessing energy, transducing it into physiologically relevant stimuli and focusing the site of action to localized subcellular compartments (Fig. 3d). For example, Au nanoparticles<sup>78</sup> and porous Si nanostructures<sup>42,79</sup> produce a photothermal effect that can be exploited for optocapacitive



neuromodulation. Coaxial p–i–n Si nanowires<sup>80</sup> or multi-layered Si membranes<sup>81</sup> yield photoelectrochemical current for wireless activation of neural cultures or brain activity. UCNPs<sup>20,82</sup> and fluorescent nanodiamonds<sup>83</sup> have been used for NIR vision and neuromodulation, and for visualizing intraneuronal transport, respectively. Other examples of wireless stimulation and sensing include the use of heat-dissipating or force-generating superparamagnetic nanoparticles<sup>84–86</sup> for ion channel modulation. These magnetic nanoparticles generate local force under a static magnetic field; however, in low-radiofrequency alternating magnetic fields, they can experience heat dissipation through relaxation processes<sup>87</sup>. Finally, quantum dots have potential as optical indicators of membrane voltage through the quantum-confined Stark effect<sup>88</sup>.

## Neural interfaces at all length scales

Below, we discuss how emerging nanotechnologies can be used to investigate neural systems across a range of biological length scales.

### Plasma membrane

At rest, the membrane potential sits at approximately  $-70$  mV and, depending on the net excitatory drive, becomes depolarized by a few millivolts for subthreshold events or by  $70$ – $120$  mV during action potential firing. These events are about  $120$  mV in amplitude at most; however, they generate large electric fields due to charge separation across a very thin geometry (Table 1). Therefore, electric-field-sensitive nanoscale devices, such as photoluminescent quantum dots, are candidates for local readout of the membrane potential<sup>89,90</sup>. In the presence of an electric field, quantum dots experience a fast redshift in their emission spectra and a decrease in photoluminescence intensity<sup>88</sup> (Fig. 4a). Although embedding nanoparticles  $60$  nm or smaller in size within vesicle bilayers has been feasible<sup>91</sup>, the ability to accommodate quantum dots into neuronal membranes remains a challenge, limiting quantum dot applications for neuroscience. For electrical readout, kinked semiconductor nanowire FETs (Fig. 4a) have been proposed as local detectors of membrane potentials and have been configured onto flexible SU-8 substrates for 3D probing<sup>36</sup>. To promote biomimetic intracellular entry, the surface of these nanowires can be modified with phospholipid coatings<sup>36</sup> and cell-penetrating peptides derived from HIV-1<sup>92</sup>. Additionally, synthetic molecular actuators<sup>74</sup> could provide the means to locally destabilize the membrane for device entry, as they can be designed with sensitivity to visible light, NIR, ultraviolet and radiofrequency<sup>93</sup>.

Regarding neuronal modulation, millisecond infrared pulses can trigger action potentials in unmodified membranes through optocapacitive photothermal effects<sup>75</sup>. In short, infrared irradiation results in local heating around the cell membrane, causing an increase in membrane capacitance ( $C$ ) that generates an inward depolarizing capacitive current ( $I_{cap}$ ). This technique explores the derivative of the capacitance that appears when one differentiates with respect to time the charge ( $Q$ ) flowing to or from the membrane capacitor, as described by



$$I_{\text{cap}} = \frac{dQ}{dt} = C \frac{dV}{dt} + V \frac{dC}{dt}$$

(3)

Au nanorods<sup>75</sup> and porous Si nanostructures<sup>42,79</sup> can also show this phenomenon, as they experience heating upon irradiation with visible and NIR wavelengths and can be surface-modified with high-avidity neuronal ligands and antibodies<sup>78</sup>. Therefore, nanostructured materials (Fig. 4a) offer a more targeted and localized photothermal stimulation, and can shift working wavelengths towards those commonly accessible in research laboratories and clinical settings<sup>78</sup>. Alternatively, researchers have begun to explore the potential use of nanostructured photodiodes<sup>80</sup> (as illustrated by the coaxial blue/green nanowire in Fig. 4a, top right) as free-standing, minimally invasive, and potentially more sensitive optoelectronic stimulators. Recently, Parameswaran et al. demonstrated that p–i–n Si nanowires doped with atomic Au on the surface exhibit photoelectrochemical current generation upon irradiation with visible light<sup>80</sup> and can elicit single and trains of action potentials. The inclusion of Au and potentially other catalysts in these nanostructures enhances the Faradaic photoelectrochemical output<sup>80,81</sup> and results in wireless activation of neuronal membranes.

### Membrane-associated proteins

Currently, 60% of all pharmacological drugs target membrane-associated proteins, mainly G-protein-coupled receptors, ligand-gated ion channels and voltage-gated ion channels<sup>94</sup>. Although the design of pharmaceuticals has been instrumental in improving human health, they can produce many off-target side effects as they access several tissues and organs. Therefore, nanoscale platforms (Fig. 4b) capable of targeting a wider array of molecular targets and modulating protein activity through a broader range of modalities could shape the future of medicine. For example, exosomes<sup>69</sup>, liposomes, polymeric nanoparticles<sup>95</sup> and DNA nanocages<sup>67</sup> can present moieties for specific cell targeting (including the location of disease pathology) and induce endocytosis. Similarly, voltage-gated ion channels can be modulated by local changes in the membrane potential, through either photoelectrochemical process by coaxial nanowires<sup>80</sup> or optocapacitive effect by Au nanoparticles<sup>75,78</sup> and porous nanostructures<sup>42,71,79</sup>. Under constant illumination, Au nanostructures, instead of driving the optocapacitive effect, can induce suppression of spontaneous and potentially evoked correlated activity, through the activation of temperature-sensitive ion channels, such as TREK1 temperature-sensitive potassium channels<sup>96</sup>. Superparamagnetic nanoparticles can also have dual roles, as either local heat generators to target temperature-sensitive ion channels, such as TRPV1, or local force generators to target mechanosensitive channels. The ability to specifically target these ion channels will shed light on the mechanisms underlying touch perception, pain sensation and regulation of internal pressure.

Furthermore, cells cultured on vertically protruding nanostructures have revealed that local membrane curvature resulting from the settling of cell membranes around vertical electrodes promotes the recruitment of membrane curvature-sensing proteins and the engulfment of

foreign particles<sup>97</sup> (Fig. 4b). Lastly, nanoprobe can work in conjunction with optogenetic ion channels, allowing researchers to obtain a better understanding of their biophysical mechanisms and to further expand their potential use in vivo. For instance, bacterial opsins reconstituted in artificial lipid bilayers can be interfaced with Si nanowire FETs; on light illumination, the flow of ions across these channels will change the local pH around the nanoFET and yield a variation in device conductance<sup>98</sup>. Moreover, in combination with UCNPs, optogenetic strategies (Fig. 4b) can be extended for deep brain stimulation, given that UCNPs can convert tissue-penetrating NIR laser pulses into visible light<sup>99</sup>.

### Subcellular organelles

In addition to biochemical signalling, mechanotransduction and charge-transfer phenomena are widespread throughout biological systems and across length scales. This is exemplified by subcellular organelles, but how these fundamental forces help coordinate subcellular processes and how they influence cell function and survival remain open ended questions in cell biology and require tools capable of visualizing and interrogating their interactions.

Nanostructures with physical features on the same order as organelles display negligible or low cytotoxicity and can enter cells through multiple internalization mechanisms<sup>97,100</sup>. For example, internalized fluorescent nanodiamond<sup>83</sup>, photoluminescent quantum dots<sup>88</sup> and engulfed Au nanorods<sup>101,102</sup> become localized in endosomes and aid real-time imaging of axonal transport in cultured neurons<sup>83</sup> (Fig. 3c). Nanoscale probes can help us to achieve a deeper understanding of biophysical mechanisms involved in molecular transport with the goal of potentially integrating these into biohybrid systems<sup>103</sup>. Organelles, such as the endoplasmic reticulum and mitochondria, may also be interfaced with photothermal Au nanoparticles<sup>78</sup> and nanostructured Si (ref. 79,81) for modulation of intracellular calcium levels and metabolic control over individual cells (Fig. 3c). However, it is important to note that the illumination condition during photothermal stimulation should be considered if reactive oxygen species and other cytotoxic effects need to be avoided<sup>104</sup>. Additionally, in cases where a strong, non-damaging photothermal effect is induced, local shockwaves can be generated by the rapid increase in temperature, which have the potential for cytoskeletal manipulation and activation of mechanosensitive proteins inside cells<sup>81</sup>. Finally, DNA nanocages can locally deliver molecular payload inside cells<sup>67</sup> and report on intracellular and luminal levels of calcium<sup>105</sup>, chloride<sup>62,65,66</sup> and pH<sup>66</sup> (Fig. 3c).

### Neurites and dendritic spines

Advances in fluorescence<sup>106–108</sup> and electron microscopy<sup>109</sup> have made it possible to map the connections of neuronal processes (or neurites) in 3D space, with nanometre resolution, across the entire nervous system of invertebrates<sup>110</sup> and many mammalian brain regions<sup>111,112</sup>. Nevertheless, how these anatomical substrates correlate to physiological function remains elusive in neuroscience, partly owing to the lack of tools able to interrogate local membrane dynamics.

Dendritic spines are membranous protrusions in dendrites, consisting of a spine head enriched in postsynaptic receptors and a narrow neck that compartmentalizes the spine from the rest of the dendrite<sup>113</sup>. Despite their extremely small size (Table 1), they play important

roles in neuronal processes such as synaptic plasticity and have been recently targeted with quantum-dot-coated nanopipettes<sup>114</sup> (Fig. 4d), revealing the dependency of somato-dendritic excitatory postsynaptic potentials on spine neck resistance. Therefore, as techniques for targeting dendrites and spines with nanoFETs and nanowire modulators<sup>79</sup> (Fig. 4d) become more readily available, we expect that nanotechnology will open exciting opportunities to understand the electrical signals generated in dendritic structures and how they spread across neurons.

Axons also play important roles in bioelectric signalling, as action potentials generated at the axon hillock are conducted towards the axon terminal where they trigger neurotransmitter release. Nanoscale interfaces have aided in studies of axonal signal propagation using nanoFET arrays<sup>115</sup>; however, nanostructures can also be used for studying axogenesis. For example, superparamagnetic nanoparticles functionalized with TrkB antibodies (Fig. 4d) have proven to be beneficial as they can initiate neurotrophic signalling and become engulfed into signalling endosomes<sup>116</sup>. Once located inside endosomes, these functionalized magnetic nanoparticles can help to visualize endosomes as they travel throughout neurons, and provide a means of manipulating endosome position and the neurite growth dynamics through the application of magnetic fields<sup>116</sup>.

### Intercellular junctions

Neural communication is a fast and dynamic process coordinated by molecularly defined synaptic junctions, where the activity of a presynaptic neuron influences the activity of its postsynaptic neuron(s). During development, growth cones sense molecular guidance cues in the extracellular environment that direct their growth towards appropriate sublaminae where synaptic partners meet and form synapses. However, studies have recently demonstrated that nanowire topography<sup>117</sup> also carries relevant information that helps guide neurite growth and coordinate synapse formation (Fig. 5a), suggesting that the nanoscale architecture of the extracellular environment works together with chemical cues to direct neurites to their proper destination. Further studies focusing on how nanoscale topography can be used to replicate neuronal organization seen in vivo will lead to advances in 3D neuron cultures and brain organoid research (Fig. 2c,d). Moreover, techniques for interrogating and manipulating synapses are highly desirable in neuroscience research, as these can help to test functional connections between neurons and determine the contribution of specific synapses to neuronal output. Free-standing nanoscale devices, such as intracellular Si nanowires<sup>81</sup> and extracellular Au particles<sup>78,96</sup>, are inorganic alternatives for intercellular neuromodulation (Fig. 5a) that can interface neurons and synapses inaccessible through genetic strategies.

In addition to synaptic junctions, neurons form intercellular junctions with multiple glial types (Fig. 5a), including astrocytes, oligodendrocytes in the central nervous system (CNS), and Schwann cells in the peripheral nervous system (PNS). Astrocytes form intimate associations with the synaptic structure (Fig. 1e) regulating neural activity through local ion buffering<sup>118</sup> and neurotransmitter uptake<sup>119</sup>. Therefore, by interfacing with astrocytic networks, nanoscale devices can potentially manipulate neural communication locally and over extended brain areas. On the other hand, myelin-forming glia — oligodendrocytes in

the CNS and Schwann cells in the PNS — wrap around and insulate axons. These myelinated segments are interrupted by uninsulated hotspots highly concentrated in voltage-gated  $\text{Na}^+$  channels called nodes of Ranvier (Fig. 2a), where action potentials are regenerated as they travel down the axon<sup>120</sup>. Myelination allows for faster conduction of electrical signals, minimizes energy consumption, and maintains the integrity and overall health of the axon<sup>121</sup>. Understanding the precise mechanisms by which axons become myelinated is crucial to establishing strategies for promoting remyelination following injury, after onset of demyelinating diseases (such as multiple sclerosis), and for building new ‘myelinated’ bioelectronics. Earlier work using electrospun nanofibre and micropillar arrays (Fig. 5a) demonstrated that axon diameter plays an important role in oligodendrocyte targeting and the initiation of myelin wrapping<sup>122,123</sup>. Moreover, activity-dependent signalling between neurons and oligodendrocytes has been shown to contribute to the myelination process<sup>124</sup>, opening the possibility for bioelectronic devices as therapeutic agents for remyelination.

### Blood–brain barrier

A challenge in treating neurological disorders is the delivery of pharmaceutical drugs from the circulatory system into the brain. Endothelial cells lining blood vessels passing through the brain, along with astrocytes and pericytes, form the blood–brain barrier (BBB), a collection of tight junctions that restrict the movement of large molecules from blood into neural tissue (Fig. 5b). Advanced drug delivery systems, such as polymer<sup>95</sup> and magnetic<sup>125</sup> nanoparticles, can enhance transport across the BBB through receptor-mediated endocytosis. Exosomes, or extracellular vesicles secreted by cells<sup>69,126</sup>, can also be prepared to carry therapeutic agents, and studies have shown that these drug-loaded vesicles can cross the BBB through similar endocytic pathways. Other approaches have focused on strategies capable of reversibly permeabilizing the BBB without causing any permanent cell damage. For instance, local heat generation with magnetothermal nanoparticles<sup>125</sup> and electroporation<sup>127</sup> can transiently increase BBB permeability and allow drugs to diffuse into the brain. Bioelectronic devices (Fig. 5b), such as mesh nanoelectronic scaffolds<sup>46</sup> and optoelectronic devices<sup>81</sup>, can be potentially used to deliver pulses of electrical current at the BBB interface for enhanced drug transport. Although animal studies are the ultimate goal when conducting tests on BBB permeability, *in vivo* experiments often result in greater experimental complexity and species-specific effects. On the other hand, *in vitro* systems allow researchers to test the nanoenabled BBB permeabilization and neural control more rapidly, using, for example, organ-on-chip platforms<sup>128</sup> (Fig. 5b). These configurations aim to create physiologically relevant microenvironments and eliminate species-specific variables. They also enable faster testing of drugs, drug delivery vehicles and devices capable of permeabilizing the BBB.

### 3D neural cultures

The extracellular matrix (ECM) is composed of a wide variety of proteins and other bioactive molecules that regulate neuronal differentiation and growth. Recently, synthetic ECM or ECM-like devices (Fig. 5c) have been explored for regulating and interrogating 3D neuronal growth and function<sup>68,129</sup>. For example, peptide amphiphile nanofibres functionalized with bioactive components<sup>68,129</sup>, such as brain-derived neurotrophic factor,

laminin and heparan sulfate epitopes, have been used to present growth factors to neurons. Interestingly, the effects of these factors on neuronal maturation and neurite growth were evident only when presented in peptide amphiphile nanofibre configurations<sup>68,129</sup>, suggesting that nanoscale architecture and topography work synergistically with the chemical nature of these molecules to initiate downstream signalling. For interrogating neural activity, folded macroporous nanoelectronic mesh devices (Fig. 5c) have generated interpenetrating recording networks with neurites, and have recorded the local field potentials and drug responses from engineered 3D neural cultures<sup>130</sup>. Additionally, ECM-like nanopores<sup>51,131</sup> developed for engineered cardiac tissues (Fig. 5c) can be extended to neuronal preparations, since electrical properties across electrogenic cells follow similar fundamental principles. Recent examples include the ultra-light and movable nanogold–polyurethane mesh electronics<sup>51,52</sup> used to monitor the electrical signals in cardiomyocytes<sup>51</sup>, and the coaxial p–i–n Si nanowire network over the self-aligned SU-8 mesh for cardiac modulation<sup>131</sup>.

### Neural systems and entire brain regions

As previously described, neurons exist within high-dimensional networks that extend over entire brain regions and perform specific tasks. Despite having individualized roles, neurons in specialized brain regions work in unity to generate, process and relay information. Therefore, the seamless interrogation of large ensembles of neurons is vital for understanding the information represented in neural systems, correlating signals to specific behaviours and monitoring how neural activity changes during disease progression. Additionally, the ability to modulate neural activity at the systems level can have multiple clinical implications, including terminating the spread of seizures, alleviating motor symptoms in Parkinson's disease patients and potentially slowing neurodegeneration in Alzheimer's disease. Advances in micro- and nanofabrication have led to the design and realization of new high-density transistor platforms for neural biointerfaces with the capability of resolving individual cells. For example, mesh nanoelectronics<sup>130</sup> (Fig. 5d) can be used for both modulation and recording of neural activity and their enhanced flexibility enables their packaging into small injection vehicles for subcortical brain delivery<sup>10,46</sup>. Following release, mesh nanoelectronics devices can form intimate contacts with neuronal populations<sup>9,46</sup> and enable recordings in freely behaving animals<sup>132,9</sup> with single-cell resolution (Fig. 1b).

For certain applications, transient interfaces are favourable, as they eliminate the need for surgical removal when no longer needed. In particular, bioresorbable Si nanomembranes (Fig. 5d) have been designed as effective probes for temperature, pressure and electrical activity<sup>41</sup>, enabling monitoring of post-surgery health and recovery. Other configurations include Au-decorated p–i–n Si nanomembranes (Fig. 5d) as *in vivo* optoelectronic devices for neural stimulation<sup>81</sup>. For use in combination with other optical methods, such as fluorescence imaging and optogenetics, graphene nanoelectronics (Fig. 5d) offer a transparent alternative to metals and semiconductors while maintaining suitable signal sensitivity<sup>17,43</sup>.

The 2D structure of Si nanomembranes and graphene microelectrodes limits their use to superficial cortical layers. However, deep brain interrogation can be achieved with superparamagnetic nanoparticles and UCNPs (Fig. 5d), because these can be wirelessly activated and can be delivered through injectable methods or potentially through the blood by transiently permeabilizing the BBB. Magnetic fields have excellent penetration through the skull and soft tissue, making magnetic nanoparticles extremely useful for deep brain magnetothermal stimulation<sup>133,134</sup>. Additionally, UCNPs can respond to NIR lasers, which also exhibit good tissue penetration. Upon NIR laser stimulation, UCNPs become excited and emit light in the visible range, which can modulate light-gated opsins<sup>99</sup> and potentially other optoelectronic nanomaterials for deep brain stimulation. Lastly, acoustically modulated gas-filled protein vesicles have been used as high-contrast agents for deep-brain MRI<sup>70,135</sup>, and rectennas (rectifying antennas) capable of harvesting high-frequency electromagnetic radiation can offer wireless control of implanted nanoprobe using Wi-Fi signals<sup>12</sup>.

## Conclusion and outlook

As illustrated throughout this Review, advances in nanotechnology offer the capability of interfacing the brain with unprecedented resolution. The seamless integration of next-generation probes with the nervous system will shed light on many unanswered questions in neuroscience, re-evaluate some principles believed to be understood, and aid in therapeutics aiming to restore proper brain function. On the other hand, future rational design and implementation of nanoscale neural devices should be guided by the physical properties of neural components and their networks (Table 1). For example, to achieve ‘myelinated’ mesh nanoelectronic devices for modulating oligodendrocyte behaviour, the diameter/width of the mesh filament should not be less than 0.4  $\mu\text{m}$  (ref. <sup>122</sup>). Efforts in optimizing these devices are still ongoing, but successes in wireless interfacing<sup>80,136</sup> and restoring or enhancing perceptual sensation<sup>18,20</sup> show that we are already at the initial stages of the nano-revolution in neuroscience.

The materials and devices described here minimize the mechanical and feature-size mismatch between probes and biological tissue. However, challenges remain for delivery and targeting, especially when precision electronic medicine<sup>137</sup> is envisaged. In particular, the skull represents a major obstacle for device implantation, often requiring invasive drilling or surgery. Interestingly, the presence of transcortical vessels that penetrate through the skull, connecting the bone marrow to the surface of the brain, has been recently reported<sup>138</sup>. These vessels could be exploited as avenues to enable deep brain interfaces for recording and modulation, although new engineering strategies will be necessary to target the desired brain regions with minimal harm. Furthermore, neural devices will require surface functionalization with cell- or subcellular-specific molecules that can enable tight junctions with molecularly defined populations. This will require close collaboration with molecular biologists researching transcriptomic and proteomic neural libraries and cell-type specific markers.

Nanoscale building blocks continue to be scaled down towards the order of organelles and protein complexes, blurring the distinction between neural interfaces and synthetic biology. At subcellular and molecular scales, bioelectronics could potentially enable real-time control



of biological circuits involved in gene expression, regulatory networks and metabolism, among others<sup>139</sup>. Such biohybrid systems can be designed and engineered so that biological systems develop a symbiotic relationship with materials or implants, allowing them both to act as integral device components. This concept can be extended to neural systems for harnessing bio-energy and sustaining active neural interfaces. We envisage platforms in which the glial cells function together with the implanted materials as one hybrid system. In particular, gap-junction coupled astrocytes form networks that span large areas of the brain<sup>118,119</sup> and are known to regulate synaptic transmission locally. Therefore, modulation of the astrocytic network through nanoscale tools would allow the simultaneous modulation of local circuits and large brain areas with minimal abiological components. Furthermore, such electrode–glia systems could transform the generic excitatory stimulus coming from the inorganic electrode into a specific signal that recruits an intrinsic neuronal pathway.

## Acknowledgements

B.T. acknowledges support of this work by the Air Force Office of Scientific Research (AFOSR FA9550-18-1-0503), US Army Research Office (W911NF-18-1-0042), US Office of Naval Research (N000141612530, N000141612958) and the National Institutes of Health (NIH NS101488). W.W. acknowledges the National Institutes of Health (1R01NS109990-01). H.A.L. is supported by the National Institutes of Health (F31 EY029156-01A1). F.B. acknowledges the National Institutes of Health (R01-GM030376 and R21-EY027101).

## References

1. Boyden ES, Zhang F, Bamberg E, Nagel G & Deisseroth K Millisecond-timescale, genetically targeted optical control of neural activity. *Nat. Neurosci* 8, 1263–1268 (2005). [PubMed: 16116447]
2. Benabid AL Deep brain stimulation for Parkinson’s disease. *Curr. Opin. Neurobiol* 13, 696–706 (2003). [PubMed: 14662371]
3. Terem I et al. Revealing sub-voxel motions of brain tissue using phase-based amplified MRI (aMRI). *Magn. Reson. Med* 80, 2549–2559 (2018). [PubMed: 29845645]
4. Salatino JW, Ludwig KA, Kozai TDY & Purcell EK Glial responses to implanted electrodes in the brain. *Nat. Biomed. Eng* 1, 862–877 (2017). [PubMed: 30505625]
5. Insel TR, Landis SC & Collins FS Research priorities. The NIH BRAIN Initiative. *Science* 340, 687–688 (2013). [PubMed: 23661744]
6. Amunts K et al. The Human Brain Project: creating a European research infrastructure to decode the human brain. *Neuron* 92, 574–581 (2016). [PubMed: 27809997]
7. Poo MM et al. China Brain Project: basic neuroscience, brain diseases, and brain-inspired computing. *Neuron* 92, 591–596 (2016). [PubMed: 27809999]
8. Lacour SP, Courtine G & Guck J Materials and technologies for soft implantable neuroprostheses. *Nat. Rev. Mater* 1, 16063 (2016).
9. Yang X et al. Bioinspired neuron-like electronics. *Nat. Mater* 18, 510–517 (2019). [PubMed: 30804509]
10. Zhou T et al. Syringe-injectable mesh electronics integrate seamlessly with minimal chronic immune response in the brain. *Proc. Natl Acad. Sci. USA* 114, 5894–5899 (2017). [PubMed: 28533392]
11. Phillips R & Quake SR The biological frontier of physics. *Phys. Today* 59, 38–43 (2006).
12. Zhang X et al. Two-dimensional MoS<sub>2</sub>-enabled flexible rectenna for Wi-Fi-band wireless energy harvesting. *Nature* 566, 368–372 (2019). [PubMed: 30692651]
13. Shi Z, Graber ZT, Baumgart T, Stone HA & Cohen AE Cell membranes resist flow. *Cell* 175, 1769–1779 (2018). [PubMed: 30392960]
14. Huberman AD, Murray KD, Warland DK, Feldheim DA & Chapman B Ephrin-As mediate targeting of eye-specific projections to the lateral geniculate nucleus. *Nat. Neurosci* 8, 1013–1021 (2005). [PubMed: 16025110]



15. Dhande OS et al. Development of single retinofugal axon arbors in normal and beta2 knock-out mice. *J. Neurosci* 31, 3384–3399 (2011). [PubMed: 21368050]
16. Hoon M, Okawa H, Della Santina L & Wong RO Functional architecture of the retina: development and disease. *Prog. Retin. Eye Res* 42, 44–84 (2014). [PubMed: 24984227]
17. Choi C et al. Human eye-inspired soft optoelectronic device using high-density MoS<sub>2</sub>-graphene curved image sensor array. *Nat. Commun* 8, 1664 (2017). [PubMed: 29162854]
18. Tang J et al. Nanowire arrays restore vision in blind mice. *Nat. Commun* 9, 786 (2018). [PubMed: 29511183]
19. Dai X, Hong G, Gao T & Lieber CM Mesh nanoelectronics: seamless integration of electronics with tissues. *Acc. Chem. Res* 51, 309–318 (2018). [PubMed: 29381054]
20. Ma Y et al. Mammalian near-infrared image vision through injectable and self-powered retinal nanoantennae. *Cell* 177, 243–255 (2019). [PubMed: 30827682]
21. Millet LJ & Gillette MU Over a century of neuron culture: from the hanging drop to microfluidic devices. *Yale J. Biol. Med* 85, 501–521 (2012). [PubMed: 23239951]
22. Seabrook TA, Burbridge TJ, Crair MC & Huberman AD Architecture, function, and assembly of the mouse visual system. *Annu. Rev. Neurosci* 40, 499–538 (2017). [PubMed: 28772103]
23. Park JW, Vahidi B, Taylor AM, Rhee SW & Jeon NL Microfluidic culture platform for neuroscience research. *Nat. Protoc* 1, 2128–2136 (2006). [PubMed: 17487204]
24. Park J, Koito H, Li J & Han A Microfluidic compartmentalized co-culture platform for CNS axon myelination research. *Biomed. Microdevices* 11, 1145–1153 (2009). [PubMed: 19554452]
25. Quadrato G et al. Cell diversity and network dynamics in photosensitive human brain organoids. *Nature* 545, 48–53 (2017). [PubMed: 28445462]
26. Sloan SA, Andersen J, Pasca AM, Birey F & Pasca SP Generation and assembly of human brain region-specific three-dimensional cultures. *Nat. Protoc* 13, 2062–2085 (2018). [PubMed: 30202107]
27. Pasca AM et al. Functional cortical neurons and astrocytes from human pluripotent stem cells in 3D culture. *Nat. Methods* 12, 671–678 (2015). [PubMed: 26005811]
28. Birey F et al. Assembly of functionally integrated human forebrain spheroids. *Nature* 545, 54–59 (2017). [PubMed: 28445465]
29. Kato-Negishi M, Morimoto Y, Onoe H & Takeuchi S Millimeter-sized neural building blocks for 3D heterogeneous neural network assembly. *Adv. Healthc. Mater* 2, 1564–1570 (2013). [PubMed: 23828857]
30. Eiraku M et al. Self-organizing optic-cup morphogenesis in three-dimensional culture. *Nature* 472, 51–56 (2011). [PubMed: 21475194]
31. Lancaster MA et al. Guided self-organization and cortical plate formation in human brain organoids. *Nat. Biotechnol.* 35, 659–666 (2017). [PubMed: 28562594]
32. Jiang YW & Tian BZ Inorganic semiconductor biointerfaces. *Nat. Rev. Mater* 3, 473–490 (2018).
33. Fu TM et al. Sub-10-nm intracellular bioelectronic probes from nanowire–nanotube heterostructures. *Proc. Natl Acad. Sci. USA* 111, 1259–1264 (2014). [PubMed: 24474745]
34. Mirza MM et al. One dimensional transport in silicon nanowire junction-less field effect transistors. *Sci. Rep* 7, 3004 (2017). [PubMed: 28592820]
35. Colinge J-P et al. Nanowire transistors without junctions. *Nat. Nanotechnol* 5, 225–229 (2010). [PubMed: 20173755]
36. Tian B et al. Three-dimensional, flexible nanoscale field-effect transistors as localized bioprobes. *Science* 329, 830–834 (2010). [PubMed: 20705858]
37. Zhao Y et al. Shape-controlled deterministic assembly of nanowires. *Nano Lett.* 16, 2644–2650 (2016). [PubMed: 26999059]
38. Duan X et al. Intracellular recordings of action potentials by an extracellular nanoscale field-effect transistor. *Nat. Nanotechnol* 7, 174–179 (2011). [PubMed: 22179566]
39. Gao RX et al. Outside looking in: nanotube transistor intracellular sensors. *Nano Lett.* 12, 3329–3333 (2012). [PubMed: 22583370]
40. Cohen-Karni T et al. Synthetically encoded ultrashort-channel nanowire transistors for fast, pointlike cellular signal detection. *Nano Lett* 12, 2639–2644 (2012). [PubMed: 22468846]

41. Kang SK et al. Bioresorbable silicon electronic sensors for the brain. *Nature* 530, 71–76 (2016). [PubMed: 26779949]
42. Jiang Y et al. Heterogeneous silicon mesostructures for lipid-supported bioelectric interfaces. *Nat. Mater* 15, 1023–1030 (2016). [PubMed: 27348576]
43. Park DW et al. Graphene-based carbon-layered electrode array technology for neural imaging and optogenetic applications. *Nat. Commun* 5, 5258 (2014). [PubMed: 25327513]
44. Kuzum D et al. Transparent and flexible low noise graphene electrodes for simultaneous electrophysiology and neuroimaging. *Nat. Commun* 5, 5259 (2014). [PubMed: 25327632]
45. Tian B et al. Macroporous nanowire nanoelectronic scaffolds for synthetic tissues. *Nat. Mater* 11, 986–994 (2012). [PubMed: 22922448]
46. Liu J et al. Syringe-injectable electronics. *Nat. Nanotechnol* 10, 629–636 (2015). [PubMed: 26053995]
47. Xie C et al. Three-dimensional macroporous nanoelectronic networks as minimally invasive brain probes. *Nat. Mater.* 14, 1286–1292 (2015). [PubMed: 26436341]
48. Xu J et al. Highly stretchable polymer semiconductor films through the nanoconfinement effect. *Science* 355, 59–64 (2017). [PubMed: 28059762]
49. Fu TM, Hong G, Viveros RD, Zhou T & Lieber CM Highly scalable multichannel mesh electronics for stable chronic brain electrophysiology. *Proc. Natl Acad. Sci. USA* 114, E10046–E10055 (2017). [PubMed: 29109247]
50. Koo J et al. Wireless bioresorbable electronic system enables sustained nonpharmacological neuroregenerative therapy. *Nat. Med* 24, 1830–1836 (2018). [PubMed: 30297910]
51. Lee S et al. Ultrasoft electronics to monitor dynamically pulsing cardiomyocytes. *Nat. Nanotechnol* 14, 156–160 (2019). [PubMed: 30598525]
52. Miyamoto A et al. Inflammation-free, gas-permeable, lightweight, stretchable on-skin electronics with nanomeshes. *Nat. Nanotechnol.* 12, 907–913 (2017). [PubMed: 28737748]
53. Hai A, Shappir J & Spira ME In-cell recordings by extracellular microelectrodes. *Nat. Methods* 7, 200–202 (2010). [PubMed: 20118930]
54. Hai A & Spira ME On-chip electroporation, membrane repair dynamics and transient in-cell recordings by arrays of gold mushroom-shaped microelectrodes. *Lab Chip* 12, 2865–2873 (2012). [PubMed: 22678065]
55. Xie C, Lin Z, Hanson L, Cui Y & Cui B Intracellular recording of action potentials by nanopillar electroporation. *Nat. Nanotechnol* 7, 185–190 (2012). [PubMed: 22327876]
56. Lin ZC, Xie C, Osakada Y, Cui Y & Cui B Iridium oxide nanotube electrodes for sensitive and prolonged intracellular measurement of action potentials. *Nat. Commun* 5, 3206 (2014). [PubMed: 24487777]
57. Robinson JT et al. Vertical nanowire electrode arrays as a scalable platform for intracellular interfacing to neuronal circuits. *Nat. Nanotechnol* 7, 180–184 (2012). [PubMed: 22231664]
58. Dipalo M et al. Intracellular and extracellular recording of spontaneous action potentials in mammalian neurons and cardiac cells with 3D plasmonic nanoelectrodes. *Nano Lett.* 17, 3932–3939 (2017). [PubMed: 28534411]
59. Dipalo M et al. Plasmonic meta-electrodes allow intracellular recordings at network level on high-density CMOS-multi-electrode arrays. *Nat. Nanotechnol* 13, 965–971 (2018). [PubMed: 30104618]
60. Luan L et al. Ultraflexible nanoelectronic probes form reliable, glial scar-free neural integration. *Science Advances* 3, e1601966 (2017). [PubMed: 28246640]
61. Gonzales DL et al. Scalable electrophysiology in intact small animals with nanoscale suspended electrode arrays. *Nat. Nanotechnol.* 12, 684–691 (2017). [PubMed: 28416816]
62. Saha S, Prakash V, Halder S, Chakraborty K & Krishnan Y A pH-independent DNA nanodevice for quantifying chloride transport in organelles of living cells. *Nat. Nanotechnol* 10, 645–651 (2015). [PubMed: 26098226]
63. Thubagere AJ et al. A cargo-sorting DNA robot. *Science* 357, eaan6558 (2017). [PubMed: 28912216]

64. Bhatia D et al. Quantum dot-loaded monofunctionalized DNA icosahedra for single-particle tracking of endocytic pathways. *Nat. Nanotechnol* 11, 1112–1119 (2016). [PubMed: 27548358]
65. Prakash V, Saha S, Chakraborty K & Krishnan Y Rational design of a quantitative, pH-insensitive, nucleic acid based fluorescent chloride reporter. *Chem. Sci* 7, 1946–1953 (2016). [PubMed: 30050672]
66. Leung K, Chakraborty K, Saminathan A & Krishnan YA DNA nanomachine chemically resolves lysosomes in live cells. *Nat. Nanotechnol* 14, 176–183 (2019). [PubMed: 30510277]
67. Veetil AT et al. Cell-targetable DNA nanocapsules for spatiotemporal release of caged bioactive small molecules. *Nat. Nanotechnol.* 12, 1183–1189 (2017). [PubMed: 28825714]
68. Edelbrock AN et al. Supramolecular nanostructure activates TrkB receptor signaling of neuronal cells by mimicking brain-derived neurotrophic factor. *Nano Lett.* 18, 6237–6247 (2018). [PubMed: 30211565]
69. Alvarez-Erviti L et al. Delivery of siRNA to the mouse brain by systemic injection of targeted exosomes. *Nat. Biotechnol.* 29, 341–345 (2011). [PubMed: 21423189]
70. Shapiro MG et al. Biogenic gas nanostructures as ultrasonic molecular reporters. *Nat. Nanotechnol* 9, 311–316 (2014). [PubMed: 24633522]
71. Sytnyk M et al. Cellular interfaces with hydrogen-bonded organic semiconductor hierarchical nanocrystals. *Nat. Commun* 8, 91 (2017). [PubMed: 28733618]
72. Tortiglione C et al. Semiconducting polymers are light nanotransducers in eyeless animals. *Sci. Adv* 3, e1601699 (2017). [PubMed: 28138549]
73. Berna J et al. Macroscopic transport by synthetic molecular machines. *Nat. Mater* 4, 704–710 (2005). [PubMed: 16127455]
74. Garcia-Lopez V et al. Molecular machines open cell membranes. *Nature* 548, 567–572 (2017). [PubMed: 28858304]
75. Carvalho-de-Souza JL, Pinto BI, Pepperberg DR & Bezanilla F Optocapacitive generation of action potentials by microsecond laser pulses of nanojoule energy. *Biophys. J* 114, 283–288 (2018). [PubMed: 29273263]
76. Kubanek J, Shukla P, Das A, Baccus SA & Goodman MB Ultrasound elicits behavioral responses through mechanical effects on neurons and ion channels in a simple nervous system. *J. Neurosci* 38, 3081–3091 (2018). [PubMed: 29463641]
77. Hallett M Transcranial magnetic stimulation and the human brain. *Nature* 406, 147–150 (2000). [PubMed: 10910346]
78. Carvalho-de-Souza JL et al. Photosensitivity of neurons enabled by cell-targeted gold nanoparticles. *Neuron* 86, 207–217 (2015). [PubMed: 25772189]
79. Fang Y et al. Texturing silicon nanowires for highly localized optical modulation of cellular dynamics. *Nano Lett.* 18, 4487–4492 (2018). [PubMed: 29894630]
80. Parameswaran R et al. Photoelectrochemical modulation of neuronal activity with free-standing coaxial silicon nanowires. *Nat. Nanotechnol* 13, 260–266 (2018). [PubMed: 29459654]
81. Jiang YW et al. Rational design of silicon structures for optically controlled multiscale biointerfaces. *Nat. Biomed. Eng* 2, 508–521 (2018). [PubMed: 30906646]
82. Pliss A et al. Subcellular optogenetics enacted by targeted nanotransformers of near-infrared light. *ACS Photonics* 4, 806–814 (2017).
83. Haziza S et al. Fluorescent nanodiamond tracking reveals intraneuronal transport abnormalities induced by brain-disease-related genetic risk factors. *Nat. Nanotechnol* 12, 322–328 (2017). [PubMed: 27893730]
84. Huang H, Delikanli S, Zeng H, Ferkey DM & Pralle A Remote control of ion channels and neurons through magnetic-field heating of nanoparticles. *Nat. Nanotechnol* 5, 602–606 (2010). [PubMed: 20581833]
85. Tay A & Di Carlo D Magnetic nanoparticle-based mechanical stimulation for restoration of mechano-sensitive ion channel equilibrium in neural networks. *Nano Lett.* 17, 886–892 (2017). [PubMed: 28094958]
86. Tay A, Kunze A, Murray C & Di Carlo D Induction of calcium influx in cortical neural networks by nanomagnetic forces. *ACS Nano* 10, 2331–2341 (2016). [PubMed: 26805612]

87. Roet M et al. Progress in neuromodulation of the brain: a role for magnetic nanoparticles? *Prog. Neurobiol* 177, 1–14 (2019). [PubMed: 30878723]
88. Efros AL et al. Evaluating the potential of using quantum dots for monitoring electrical signals in neurons. *Nat. Nanotechnol* 13, 278–288 (2018). [PubMed: 29636589]
89. Peterka DS, Takahashi H & Yuste R Imaging voltage in neurons. *Neuron* 69, 9–21 (2011). [PubMed: 21220095]
90. Marshall JD & Schnitzer MJ Optical strategies for sensing neuronal voltage using quantum dots and other semiconductor nanocrystals. *ACS Nano* 7, 4601–4609 (2013). [PubMed: 23614672]
91. Bonnaud C et al. Insertion of nanoparticle clusters into vesicle bilayers. *ACS Nano* 8, 3451–3460 (2014). [PubMed: 24611878]
92. Lee JH, Zhang A, You SS & Lieber CM Spontaneous internalization of cell penetrating peptide-modified nanowires into primary neurons. *Nano Lett.* 16, 1509–1513 (2016). [PubMed: 26745653]
93. Xu T, Gao W, Xu LP, Zhang X & Wang S Fuel-free synthetic micro-/nanomachines. *Adv. Mater* 29, 1603250 (2017).
94. Overington JP, Al-Lazikani B & Hopkins AL How many drug targets are there? *Nat. Rev. Drug Discov* 5, 993–996 (2006). [PubMed: 17139284]
95. Kreuter J Drug delivery to the central nervous system by polymeric nanoparticles: what do we know? *Adv. Drug Deliv. Rev* 71, 2–14 (2014). [PubMed: 23981489]
96. Yoo S, Hong S, Choi Y, Park JH & Nam Y Photothermal inhibition of neural activity with near-infrared-sensitive nanotransducers. *ACS Nano* 8, 8040–8049 (2014). [PubMed: 25046316]
97. Zhao W et al. Nanoscale manipulation of membrane curvature for probing endocytosis in live cells. *Nat. Nanotechnol* 12, 750–756 (2017). [PubMed: 28581510]
98. Tunuguntla RH et al. Bioelectronic light-gated transistors with biologically tunable performance. *Adv. Mater* 27, 831–836 (2015). [PubMed: 25410490]
99. Chen S et al. Near-infrared deep brain stimulation via upconversion nanoparticle-mediated optogenetics. *Science* 359, 679–683 (2018). [PubMed: 29439241]
100. Zimmerman JF et al. Cellular uptake and dynamics of unlabeled freestanding silicon nanowires. *Sci. Adv* 2, e1601039 (2016). [PubMed: 28028534]
101. Gu Y et al. Rotational dynamics of cargos at pauses during axonal transport. *Nat. Commun* 3, 1030 (2012). [PubMed: 22929787]
102. Kaplan L, Ierokomos A, Chowdary P, Bryant Z & Cui BX Rotation of endosomes demonstrates coordination of molecular motors during axonal transport. *Sci. Adv* 4, e1602170 (2018). [PubMed: 29536037]
103. Goel A & Vogel V Harnessing biological motors to engineer systems for nanoscale transport and assembly. *Nat. Nanotechnol* 3, 465–475 (2008). [PubMed: 18685633]
104. Johannsmeier S et al. Gold nanoparticle-mediated laser stimulation induces a complex stress response in neuronal cells. *Sci. Rep* 8, 6533 (2018). [PubMed: 29695746]
105. Narayanaswamy N et al. A pH-correctable, DNA-based fluorescent reporter for organellar calcium. *Nat. Methods* 16, 95–102 (2019). [PubMed: 30532082]
106. Chen F, Tillberg PW & Boyden ES Optical imaging. Expansion microscopy. *Science* 347, 543–548 (2015). [PubMed: 25592419]
107. Chung K & Deisseroth K CLARITY for mapping the nervous system. *Nat. Methods* 10, 508–513 (2013). [PubMed: 23722210]
108. Huang B, Wang W, Bates M & Zhuang X Three-dimensional super-resolution imaging by stochastic optical reconstruction microscopy. *Science* 319, 810–813 (2008). [PubMed: 18174397]
109. Denk W & Horstmann H Serial block-face scanning electron microscopy to reconstruct three-dimensional tissue nanostructure. *PLoS Biol.* 2, e329 (2004). [PubMed: 15514700]
110. Zheng Z et al. A complete electron microscopy volume of the brain of adult *Drosophila melanogaster*. *Cell* 174, 730–743 (2018). [PubMed: 30033368]
111. Martersteck EM et al. Diverse central projection patterns of retinal ganglion cells. *Cell Rep.* 18, 2058–2072 (2017). [PubMed: 28228269]
112. Gao R et al. Cortical column and whole-brain imaging with molecular contrast and nanoscale resolution. *Science* 363, eaau8302 (2019). [PubMed: 30655415]

113. Beaulieu-Laroche L & Harnett MT Dendritic spines prevent synaptic voltage clamp. *Neuron* 97, 75–82 (2018). [PubMed: 29249288]
114. Jayant K et al. Targeted intracellular voltage recordings from dendritic spines using quantum-dot-coated nanopipettes. *Nat. Nanotechnol* 12, 335–342 (2017). [PubMed: 27941898]
115. Patolsky F et al. Detection, stimulation, and inhibition of neuronal signals with high-density nanowire transistor arrays. *Science* 313, 1100–1104 (2006). [PubMed: 16931757]
116. Steketee MB et al. Nanoparticle-mediated signaling endosome localization regulates growth cone motility and neurite growth. *Proc. Natl Acad. Sci. USA* 108, 19042–19047 (2011). [PubMed: 22065745]
117. Gautam V et al. Engineering highly interconnected neuronal networks on nanowire scaffolds. *Nano Lett.* 17, 3369–3375 (2017). [PubMed: 28437614]
118. Allen NJ & Lyons DA Glia as architects of central nervous system formation and function. *Science* 362, 181–185 (2018). [PubMed: 30309945]
119. Deemyad T, Luthi J & Spruston N Astrocytes integrate and drive action potential firing in inhibitory subnetworks. *Nat. Commun* 9, 4336 (2018). [PubMed: 30337521]
120. Kandel ER *Principles of Neural Science*, 5th edn (McGraw-Hill, 2013).
121. Nave KA Myelination and support of axonal integrity by glia. *Nature* 468, 244–252 (2010). [PubMed: 21068833]
122. Lee S et al. A culture system to study oligodendrocyte myelination processes using engineered nanofibers. *Nat. Methods* 9, 917–922 (2012). [PubMed: 22796663]
123. Lee S, Chong SYC, Tuck SJ, Corey JM & Chan JR A rapid and reproducible assay for modeling myelination by oligodendrocytes using engineered nanofibers. *Nat. Protoc* 8, 771–782 (2013). [PubMed: 23589937]
124. Fields RD A new mechanism of nervous system plasticity: activity-dependent myelination. *Nat. Rev. Neurosci* 16, 756–767 (2015). [PubMed: 26585800]
125. Chen Y & Liu LH Modern methods for delivery of drugs across the blood–brain barrier. *Adv. Drug Deliv. Rev* 64, 640–665 (2012). [PubMed: 22154620]
126. Yang TZ et al. Exosome delivered anticancer drugs across the blood–brain barrier for brain cancer therapy in *Danio rerio*. *Pharm. Res* 32, 2003–2014 (2015). [PubMed: 25609010]
127. Bonakdar M, Wasson EM, Lee YW & Davalos RV Electroporation of brain endothelial cells on chip toward permeabilizing the blood–brain barrier. *Biophys. J* 110, 503–513 (2016). [PubMed: 26789772]
128. Bonakdar M, Graybill PM & Davalos RV A microfluidic model of the blood–brain barrier to study permeabilization by pulsed electric fields. *RSC Adv.* 7, 42811–42818 (2017). [PubMed: 29308191]
129. Mammadov B, Mammadov R, Guler MO & Tekinay AB Cooperative effect of heparan sulfate and laminin mimetic peptide nanofibers on the promotion of neurite outgrowth. *Acta Biomater.* 8, 2077–2086 (2012). [PubMed: 22342826]
130. Tian BZ et al. Macroporous nanowire nanoelectronic scaffolds for synthetic tissues. *Nat. Mater* 11, 986–994 (2012). [PubMed: 22922448]
131. Parameswaran R et al. Optical stimulation of cardiac cells with a polymer-supported silicon nanowire matrix. *Proc. Natl Acad. Sci.* 116, 413–421 (2019). [PubMed: 30538202]
132. Hong G et al. A method for single-neuron chronic recording from the retina in awake mice. *Science* 360, 1447–1451 (2018). [PubMed: 29954976]
133. Munshi R et al. Magnetothermal genetic deep brain stimulation of motor behaviors in awake, freely moving mice. *Elife* 6, e27069 (2017). [PubMed: 28826470]
134. Chen R, Romero G, Christiansen MG, Mohr A & Anikeeva P Wireless magnetothermal deep brain stimulation. *Science* 347, 1477–1480 (2015). [PubMed: 25765068]
135. Lu GJ et al. Acoustically modulated magnetic resonance imaging of gas-filled protein nanostructures. *Nat. Mater* 17, 456–463 (2018). [PubMed: 29483636]
136. Seo D et al. Wireless recording in the peripheral nervous system with ultrasonic neural dust. *Neuron* 91, 529–539 (2016). [PubMed: 27497221]

137. Tian BZ & Lieber CM Nanowired bioelectric interfaces. *Chem. Rev* 10.1021/acs.chemrev.8b00795 (2019).
138. Herisson F et al. Direct vascular channels connect skull bone marrow and the brain surface enabling myeloid cell migration. *Nat. Neurosci* 21, 1209–1217 (2018). [PubMed: 30150661]
139. Selberg J, Gomez M & Rolandi M The potential for convergence between synthetic biology and bioelectronics. *Cell Syst.* 7, 231–244 (2018). [PubMed: 30243561]
140. Milo R & Phillips R *Cell Biology by the Numbers*, 21, 39, 159, 198, 253 (Garland Science, 2016).
141. Wang B, Grill WM & Peterchev AV Coupling magnetically induced electric fields to neurons: longitudinal and transverse activation. *Biophys. J* 115, 95–107 (2018). [PubMed: 29972816]
142. Phillips MJ & Voeltz GK Structure and function of ER membrane contact sites with other organelles. *Nat. Rev. Mol. Cell Biol* 17, 69–82 (2016). [PubMed: 26627931]
143. Millecamps S & Julien JP Axonal transport deficits and neurodegenerative diseases. *Nat. Rev. Neurosci.* 14, 161–176 (2013). [PubMed: 23361386]
144. Xu K, Zhong GS & Zhuang XW Actin, spectrin, and associated proteins form a periodic cytoskeletal structure in axons. *Science* 339, 452–456 (2013). [PubMed: 23239625]
145. Sherman DL & Brophy PJ Mechanisms of axon ensheathment and myelin growth. *Nat. Rev. Neurosci* 6, 683–690 (2005). [PubMed: 16136172]
146. Sweeney MD, Sagare AP & Zlokovic BV Blood–brain barrier breakdown in Alzheimer disease and other neurodegenerative disorders. *Nat. Rev. Neurol* 14, 133–150 (2018). [PubMed: 29377008]
147. Duvernoy H, Delon S & Vannson JL The vascularization of the human cerebellar cortex. *Brain Res. Bull* 11, 419–480 (1983). [PubMed: 6652521]
148. Nicholson C & Hrabetova S Brain extracellular space: the final frontier of neuroscience. *Biophys. J* 113, 2133–2142 (2017). [PubMed: 28755756]
149. Budday S et al. Mechanical properties of gray and white matter brain tissue by indentation. *J. Mech. Behav. Biomed. Mater* 46, 318–330 (2015). [PubMed: 25819199]



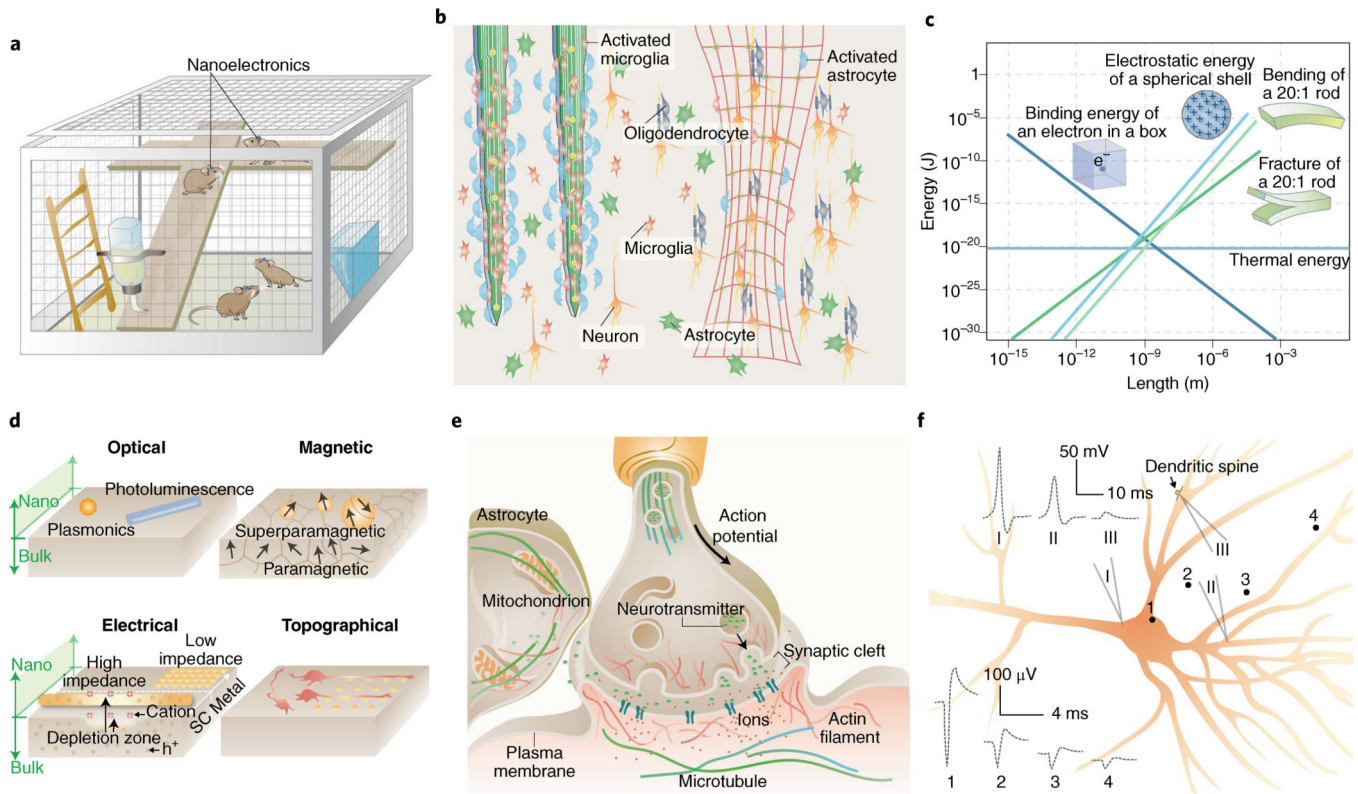


**Fig. 1 | Nanoscale materials and devices can offer new opportunities in neural interfaces.** **a**, Nanodevices offer seamless biointegration with neural components, allowing for imperceptible, minimally invasive and wireless brain interrogation. **b**, Compared with bulk implants (left), devices with nanoscale thicknesses and open framework are flexible, stretchable and can elicit less immune response (right). Many more astrocytes and microglial cells are recruited and activated at the bulk implant surfaces. **c**, Many energy terms converge in amplitude at the nanoscale, suggesting that signal transduction at the neural interfaces can take multiple forms<sup>11,140</sup>. **d**, New properties and capabilities emerge at the nanoscale. For example, as the size of metal or semiconductor shrinks, the plasmonic or photoluminescence properties exhibit size- and shape-dependency. Iron oxide switches from paramagnetic to superparamagnetic behaviour when the particle size is smaller than a single magnetic domain. FETs can be gated more easily with nanoscale channel geometries. Nanoscale protrusions or patterns can also yield a neural response that is absent for a planar neural substrate. SC, semiconductor;  $h^+$ , holes. **e**, The synaptic junction and many other subcellular domains are highly crowded, dynamic and heterogeneous. Therefore, nanoscale electrophysiology and signal transduction can differ from those recorded in the bulk. **f**, Electrical recordings show different signal shape and amplitude from different regions of a single neuron. The schematic traces 1–4 are extracellular electrical recordings from points 1–4; traces I–III are intracellular recordings from micropipettes I–III. Adapted from: **c**, ref. 11, AIP; ref. 140, Taylor & Francis.



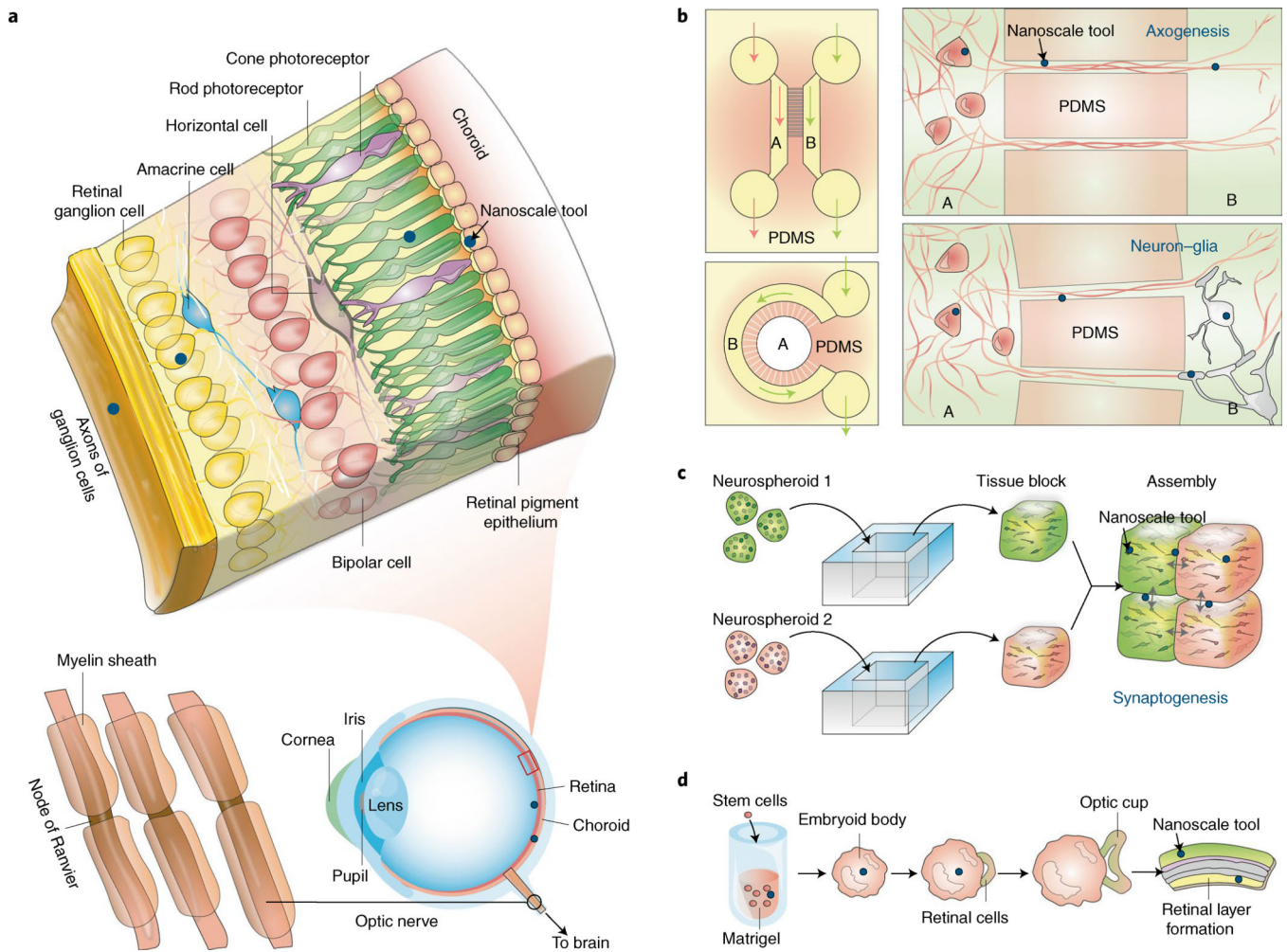


**Fig. 2 | Naturally occurring and cultured neural systems provide plenty of room for nanoscale probing.**

**a**, Layered structure of retinal tissue. Although epi- and subretinal spaces have been extensively explored for implants, nanoscale tools (blue dots) may access the retinal internal layers. **b–d**, Neural cultures in 2D and 3D can enable bottom-up integration of devices with cells in a seamless manner. **b**, Microfluidic systems with different compartments (for example, A and B) allow selective manipulation of neural cells, where nanoscale tools (blue dots) can be rationally positioned for studying axogenesis and neuron–glia interactions. **c**, Neurospheroids can be assembled into 3D tissues, and nanoscale tools (blue dots) can be positioned at the tissue block interfaces for synaptogenesis and circuit studies. **d**, Embryonic stem cells can develop into lab-grown retina, during which nanoscale tools may be used for growth control or for probing the functions of the final engineered tissues.

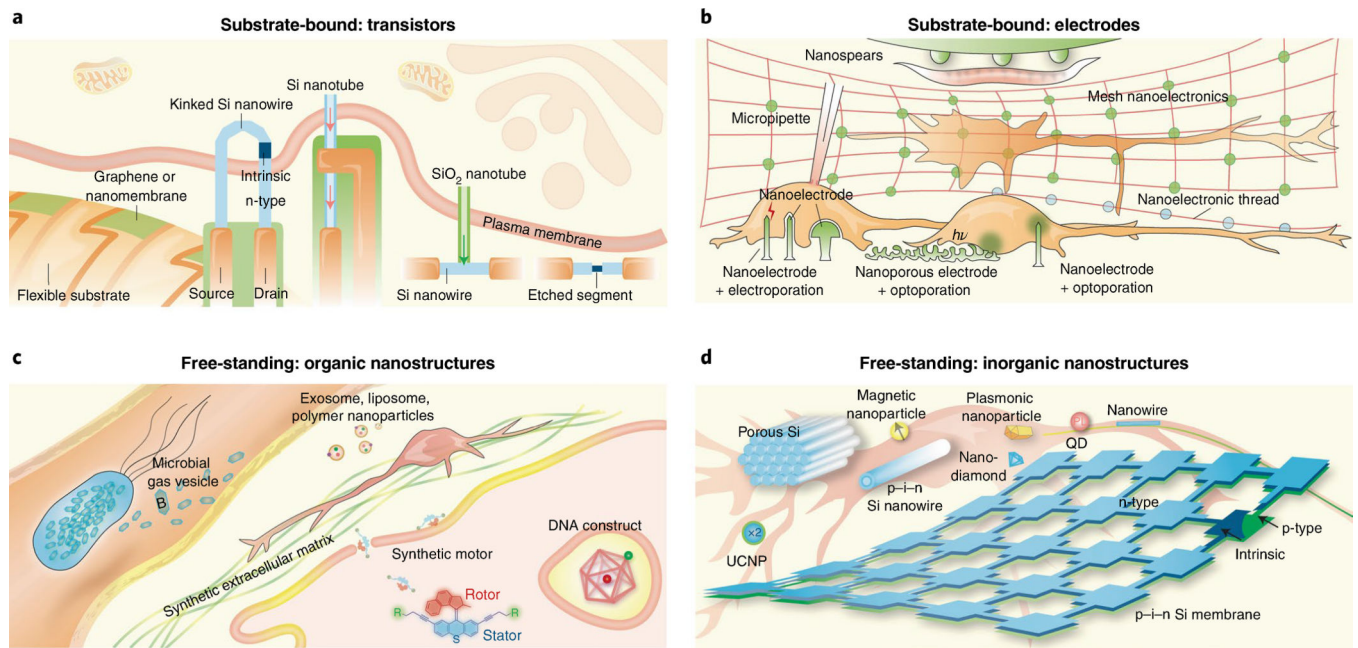


**Fig. 3 |. Nanoscale toolbox for neural interfaces.**

**a**, Sharp protrusions formed by kinked n-i-n Si nanowires, Si nanotubes, or structures with SiO<sub>2</sub> nanotube branches and Si nanowire backbones have enabled transistor-based intracellular electrical recording. Selective etching of a segment in a Si nanowire FET promises localized extracellular recording. 2D nanomaterial-based FETs over flexible substrates can form compliant extracellular biointerfaces. The arrows highlight the entrance of cytosol into FET regions. **b**, Gold mushroom-shaped nanoelectrodes, nanopillars/nanowires and nanospears yield high-resolution extracellular recording. With electroporation or optoporation, nanopillars/nanowires or nanoporous electrodes achieve intracellular recording. Metal films with nanoscale thicknesses allow brain tissue interfaces with mesh nanoelectronics or nanoelectronic-thread configurations. Nanospears represent an example of integration of a bioelectronics device with a microfluidic system. **c**, DNA constructs can be used for intracellular delivery and sensing. Synthetic ECM can guide neural differentiation and growth. Exosome, liposome, polymer nanoparticles and synthetic motors may be used for drug delivery to neurons. Recently developed microbial gas vesicles hold promise for MRI and ultrasound imaging. **d**, Mesoporous Si particles, p-i-n Si nanowires, superparamagnetic nanoparticles, plasmonics nanoparticles, UCNPs and p-i-n Si membranes have been developed for extracellular neuromodulation. The internalized Si nanowires permit intracellular modulation and cytoskeletal control. Quantum dots (QD) and nanodiamonds have been used for imaging or organelle tracking in neurons.

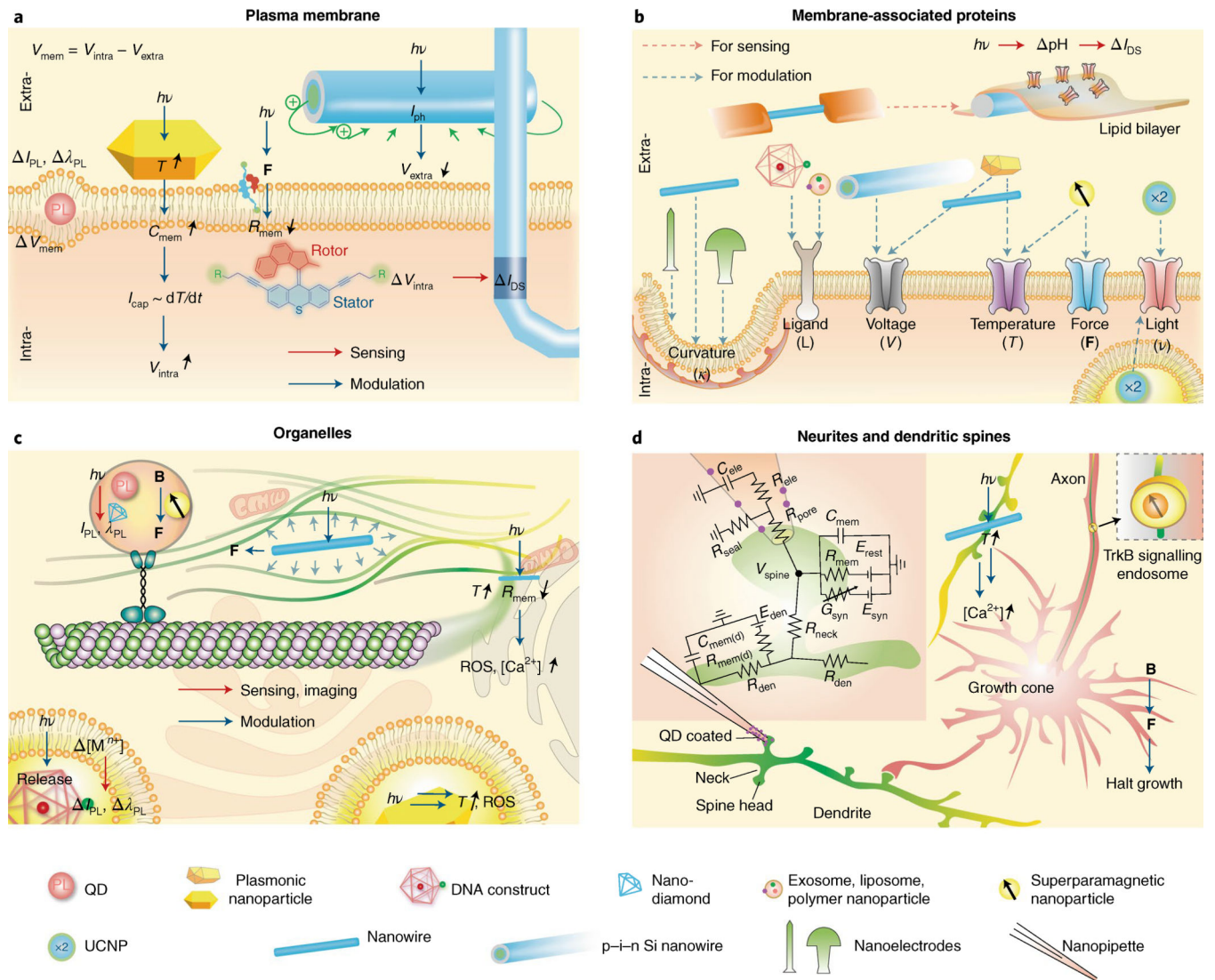


**Fig. 4 | Nano-enabled subcellular neural interfaces.**

**a**, Interfacing plasma membranes: research labs have developed kinked nanowire FETs for intracellular electrical recording, Au nanorods for photothermal neuromodulation, coaxial Si nanowires for photoelectrochemical neuromodulation, synthetic molecular rotors for potential device entrance into neurons, and quantum dots for potential optical recording of membrane voltage.  $h\nu$ , photon energy; PL, photoluminescence;  $I_{\text{PL}}$ , PL intensity change;  $\lambda_{\text{PL}}$ , PL wavelength change;  $T$ , temperature;  $F$ , force;  $I_{\text{cap}}$ , capacitive current;  $I_{\text{ph}}$ , photocurrent;  $I_{\text{DS}}$ , FET source–drain current change;  $C_{\text{mem}}$ , membrane capacitance;  $R_{\text{mem}}$ , membrane resistance;  $V_{\text{mem}}$ , membrane voltage;  $V_{\text{extra}}$ , extracellular potential;  $V_{\text{intra}}$ , intracellular potential. **b**, Interfacing membrane-associated proteins: exosomes, liposomes, polymer nanoparticles and DNA constructs present ligands for cellular targeting and induced endocytosis. Coaxial nanowire produces a photoelectrochemical effect to modulate the local extracellular potential and affects voltage-sensitive ion channels. A rapid photothermal effect from plasmonic nanoparticles or Si nanowires causes depolarization of plasma membrane and triggers activities in voltage-sensitive ion channels. The long-lasting photothermal effect



and the magnetothermal effect from superparamagnetic nanoparticles can affect temperature-sensitive ion channels. Superparamagnetic nanoparticles can also actuate mechanical-sensitive ion channels. UCNPs have been used for ion channel modulation, possibly through both extra- and intracellular configuration. Other substrate-bound nanostructures can produce a response from curvature-sensing membrane proteins. Ion channels can also be reconstituted in vitro, producing electrical sensing signals in Si nanowire FET. **c**, Interfacing organelles: quantum dots or nano-diamonds, plasmonic nanoparticles and superparamagnetic nanoparticles have been used for imaging or controlling cytoskeletal transport or polymerization. Intracellular Au may produce reactive oxygen species (ROS) and other cytotoxic effects upon light illumination. DNA constructs can be used for sensing of calcium or pH in the endosomes. Intracellular Si nanowire also allows for cytoskeletal control via the photoacoustic effect or calcium initiation via the photothermal effect.  $I_{PL}$ , PL intensity;  $\lambda_{PL}$ , PL wavelength;  $\mathbf{B}$ , magnetic field;  $[M^{n+}]$ , ion concentration. **d**, Interfacing neuritis and dendritic spines: quantum-dot-coated nanopipette allowed the recording from the spine. Magnetic control of TrkB signalling can halt the neurite growth. A cross-junction between Si nanowire and filopodium produced localized calcium initiation. Inset, schematic diagram of the electrical equivalent circuit for the passive dendritic spine, adapted from ref. <sup>114</sup>.  $R_{den}$ , dendritic resistance;  $R_{ele}$ , pipette resistance;  $R_{mem}$ , passive membrane resistance of spine head;  $R_{mem(d)}$ , dendrite passive membrane resistance;  $R_{neck}$ , neck resistance;  $R_{pore}$ , pore resistance;  $R_{seal}$ , seal resistance;  $C_{ele}$ , pipette capacitance;  $C_{mem}$ , passive membrane capacitance of spine head;  $C_{mem(d)}$ , dendrite passive membrane capacitance;  $E_{syn}$ , synaptic reversal potential;  $E_{rest}$ , leak reversal potential;  $E_{den}$ , dendritic reversal potential;  $G_{syn}$ , synaptic conductance. Adapted from: **d**, ref. <sup>114</sup>, SNL.

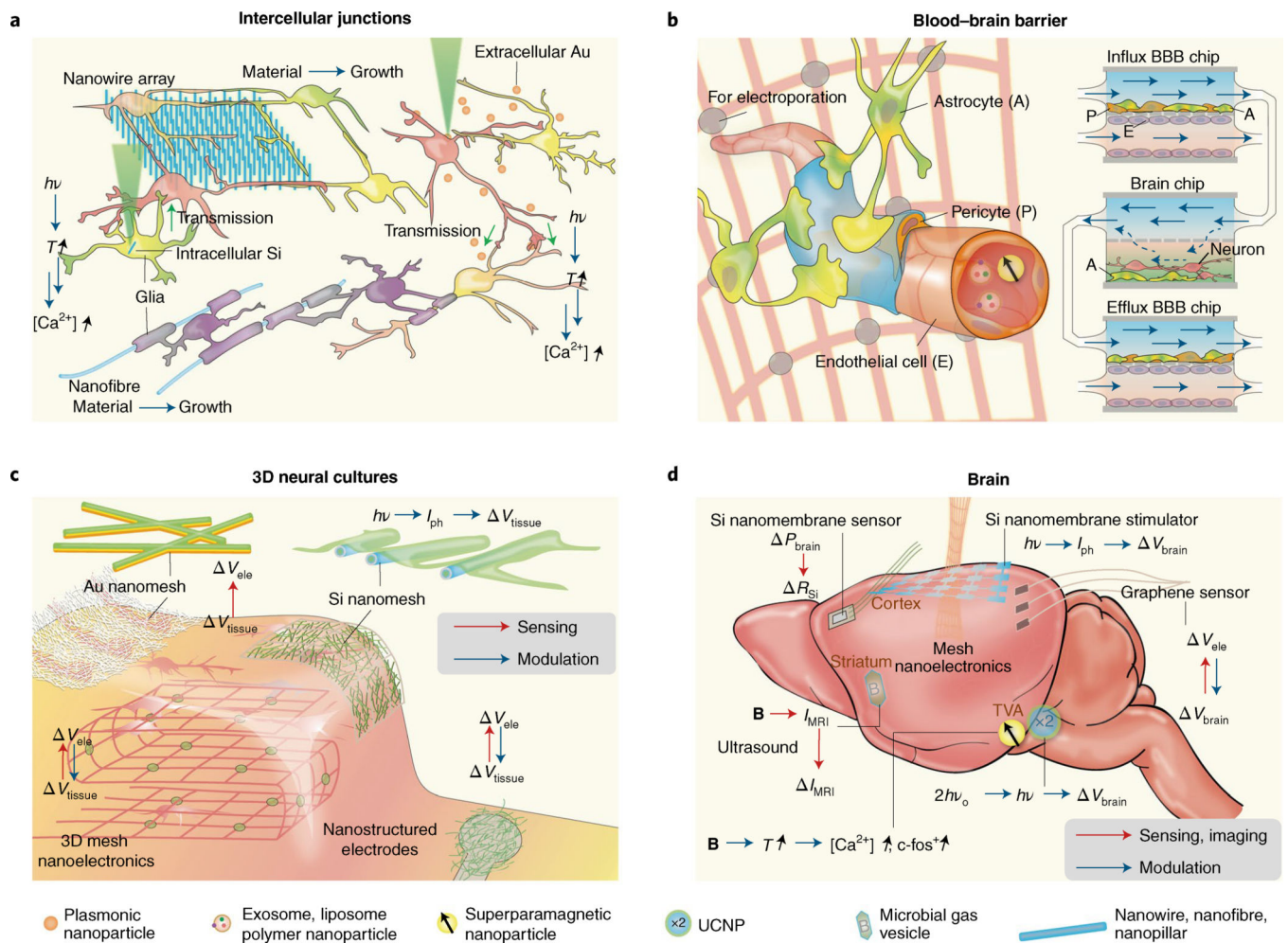


**Fig. 5 | Nano-enabled cellular and tissue-scale neural interfaces.**

**a**, Interfacing intercellular junctions. Nanowire arrays can guide neuronal processes and promote intercellular junctions and electrical synchronization. Intracellular Si or extracellular Au-based neural modulations may enable functional connection studies in neurons. Myelination of nano- and microfibres suggests future electrical or optoelectronic control of myelination through semiconductor or metallic nanowires. **b**, Interfacing the blood–brain barrier. Exosomes, liposomes, polymer nanoparticles and magnetic nanoparticles have been suggested for enhanced delivery through BBB. Future opportunities include localized electroporation through mesh nanoelectronics, given in vitro electroporation studies for enhanced BBB passage. It is also promising to include nanomaterial or nanodevices with organ-on-a-chip model where the interactions among BBB, blood and neural systems can be evaluated together. **c**, Interfacing 3D neural cultures. Macroporous nanoelectronics mesh can record from the inside of engineered tissues. Conducting nanofibre-coated recording electrodes have low impedance. Au nanomesh used for electrical recording of engineered cardiac tissues and Si nanomesh used for photoelectrochemical modulation of the heart could potentially be used for electrical interfaces with 3D neural cultures.  $V_{ele}$ , electrical potential recorded at the nanoelectronics surface;  $V_{tissue}$ , electrical potential from the tissue. **d**, Interfacing the brain. Biodegradable Si

nanomembrane can measure intracranial pressure ( $P_{\text{brain}}$ ). Si photodiode nanomembranes produce photoelectrochemical modulation of the cortex and yield a field potential change ( $V_{\text{brain}}$ ). Semi-transparent graphene electrodes allow flexible electrical recording, and parallel imaging and optical stimulation. A microbial gas vesicle produces MRI signals ( $I_{\text{MRI}}$ ) that can be modulated with ultrasound and allow multiplexed MRI imaging. Superparamagnetic nanoparticles and UCNPs yield deep-brain wireless neuromodulation, producing various effects such as the upregulation of *c-fos*, a proto-oncogene that is expressed within some neurons following depolarization.

Author Manuscript

Author Manuscript

Author Manuscript

Author Manuscript

Table 1 |

Representative numbers in neural systems that are relevant to nanoscale probing

<b>Membrane</b>	
Size	Thickness: ~5 nm Membrane disks in photoreceptor rod cells <sup>140</sup> ; disk spacing ~25 nm, disk number ~1,000
Rate	Diffusion coefficient for membrane tension <sup>13</sup> : ~0.024 $\mu\text{m}^2 \text{s}^{-1}$
Physical properties	Rupture of a membrane: ~300–400 mV (voltage <sup>140</sup> ), ~1–30 mN $\text{m}^{-1}$ (stress <sup>74</sup> ) Peak membrane electric field during an action potential <sup>88</sup> : ~250 kV $\text{cm}^{-1}$ . Membrane capacitance <sup>141</sup> : 1 $\mu\text{F cm}^{-2}$ (unmyelinated membrane), 2 $\mu\text{F cm}^{-2}$ (node of myelinated membrane), 4.2 $\times 10^{-4}$ $\mu\text{F cm}^{-2}$ (internode of myelinated membrane), Membrane resistance <sup>141</sup> : 1.48 k $\Omega \text{ cm}^2$ (unmyelinated membrane), 0.096 k $\Omega \text{ cm}^2$ (node of myelinated membrane), 240 k $\Omega \text{ cm}^2$ (internode of myelinated membrane)
<b>Ion channels</b>	
Size	~10 $\times$ 10 $\times$ 10 nm <sup>3</sup> for a voltage-gated ion channel
Rate	~10 <sup>6</sup> to 10 <sup>8</sup> ions per second
Physical properties	Time constants of activation/deactivation: submillisecond to a few milliseconds. Time constant to inactivate: tens of milliseconds to seconds or minutes. Temperature to activate TRPV1: >42 °C
<b>Organelles</b>	
Size	Synaptic vesicle volume <sup>140</sup> : ~10 <sup>-5</sup> $\mu\text{m}^3$ Gap distances at the membrane contact sites <sup>142</sup> : 3–15 nm (ER-endosome), 6–15 nm (ER-mitochondria)
Rate	Cytoskeletal transport <sup>143</sup> : ~0.3–1 $\mu\text{m s}^{-1}$ (neurofilaments, anterograde), ~0.4 $\mu\text{m s}^{-1}$ (mitochondria, bidirectional), ~0.3–0.4 $\mu\text{m s}^{-1}$ (lysosomes, bidirectional)
Physical properties	The stall forces for kinesin and dynein: ~7–8 pN (ref. 116)
Chemical properties	Neurotransmitter concentration in synaptic vesicles <sup>140</sup> : ~100–200 mM [Ca <sup>2+</sup> ] in different organelles <sup>142</sup> : ~0.5 $\mu\text{M}$ (early endosome), ~2.5 $\mu\text{M}$ (late endosome), ~100 $\mu\text{M}$ (peak concentration in inner mitochondrial matrix), ~60–500 $\mu\text{M}$ (lumen of endoplasmic reticulum), ~100 mM (nucleus)
<b>Neurites and dendritic spines</b>	
Size	Dendritic spines <sup>114</sup> ; head (volume ~0.001–0.1 $\mu\text{m}^3$ ), neck (diameter ~0.1 $\mu\text{m}$ , length ~1 $\mu\text{m}$ ) Periodicity of actin rings in axon <sup>144</sup> : ~190 nm Node of Ranvier: ~1 $\mu\text{m}$
Rate	Growth cone motility of rat retinal ganglion cell in vitro <sup>116</sup> : ~30–60 $\mu\text{m h}^{-1}$ .
Physical properties	EPSP attenuation in mouse hippocampal neuron <sup>114</sup> ; from ~26 mV (spine head) to ~0.5–1 mV (soma) Fracture strain and ultimate stress of nerves <sup>8</sup> : ~25% and ~10 MPa
<b>Intercellular junctions</b>	
Size	Chemical/electrical synaptic junction gap <sup>140</sup> : ~20–40 nm/~2–4 nm Lumen diameter of electrical gap junction channel <sup>120</sup> : ~1.2–2 nm Ratio of the axonal diameter to the diameter of the axon plus its myelin sheath (g-ratio) <sup>145</sup> : 0.6–0.7
Rate	Chemical clearance at a synapse <sup>140</sup> : ~1 ms
Physical properties	Diameter requirement for cultured oligodendrocyte myelination <sup>122</sup> : >0.4 $\mu\text{m}$



**Brain**

Size	Human brain blood vessels <sup>125,146</sup> ; number ~100 billion, length ~650 km, surface area ~10–20 m <sup>2</sup> Mean intercapillary distance in the human brain: ~40 $\mu\text{m}$ <sup>147</sup> Volume of brain extracellular space <sup>148</sup> : ~20% of the brain tissue
Rate	Action potential speeds in humans <sup>140</sup> : 10–100 m s <sup>-1</sup> Effective molecular diffusion coefficient in brain extracellular space <sup>148</sup> : ~2/5 of that in a free solution
Physical properties	Elastic modulus <sup>8,149</sup> : 1.40 kPa (grey matter), 1.90 kPa (white matter), ~0.5–1.2 MPa (dura mater), ~10 GPa (cortical bone) Elastic moduli that favour glial growth and migration <sup>8</sup> : ~700 Pa (oligodendrocytes), >10 kPa (microglia) Intracranial pressure: 7–15 mmHg